Scientific Research Publishing

Journal of High Energy Physics, Gravitation and Cosmology, 2021, 7, 1410-1424
https://www.scirp.org/journal/jhepgc
ISSN Online: 2380-4335
ISSN Print: 2380-4327

The Origin of Cosmic Structures Part 2—HI Rings

J. C. Botke

Nogales, Arizona, USA
Email: jcbotke(at)gmail.com

How to cite this paper: J. C. Botke (2021) The Origin of Cosmic Structures Part 2—HI Rings. *Journal of High Energy Physics, Gravitation and Cosmology*, **7**, 1410-1424.
https://doi.org/10.4236/jhepgc.2021.74086

Received: September 4, 2021
Accepted: October 17, 2021
Published: October 20, 2021

Abstract

Researchers have long been aware of the existence of large HI structures and over the past decades, a large observational record of their properties has been assembled. Despite all the work that has been done, however, there is no consensus about their origin. In this paper, we will show that these structures can readily be understood within the framework of a new model of cosmology based on time-varying curvature and an unconventional model of nucleosynthesis. According to this model, all galaxies came into existence at the same time during nucleosynthesis as large proton gas clouds whose detailed structure was fixed by an imprint established in the vacuum during an initial Plank inflation. One of the predictions of the model is that all these proto-galaxy gas clouds reached the zero-velocity point of their expansion with sizes many times larger than their present-day size. The large outer HI rings are simply regions of this gas that remained at the maximum size as the core compacted to its present-day size. Similarly, the inner rings are regions that did compact with the galaxy core.

Keywords

HI Rings, Galaxy Evolution, Nucleosynthesis, Early Universe, Time-Varying Curvature

1. Introduction

The problem of the HI structures has been around for a long time and up until now, no one has proposed an even plausible solution. A survey of extant scenarios is given in [1]. A common failing with these proposals is that they envision the HI structures as being the consequence of isolated events. The HI structures, however, are too common for that to be true. They are found in ~80% of the spiral galaxies and about ~40% of the lenticulars and ellipticals and that high

percentage points to a universal origin unrelated to events within or between galaxies. What we will show is that the rings came into existence as part of the galaxy formation process which began at the time of nucleosynthesis.

We will first review the observational record and then show how these observations can be understood in terms of the new model of cosmology described in [2] hereafter referred to as Part 1.

2. Brief Summary of HI Observations

In almost all cases, the HI regions are observed to be in association with host galaxies often in the form of rings (or spheres). In some cases, these are found to be positioned outside the stellar definition of the galaxy, in other cases, within, and in still other cases, in both positions. The majority of these rings are observed to be stable. The remainder have less organization and appear as scattered clouds either outside or inside the host galaxy. Finally, in a few rare cases, isolated rings or clouds have been observed that are not associated with a host galaxy.

Up until very recently, all the known outer rings were associated with optical frequency sources such as stars or star remnants which is generally thought to indicate either star formation within the ring or prior contact with some other galaxy. Recently, however, a few radio sources have been discovered that contain only a very few or no optical counterparts.

We will begin with a summary of the results of two studies based on the observation of 24 and 166 ETGs respectively. The first work, [1], is based on the observation of 24 gas-rich lenticular galaxies. The authors first describe their lenticular observations and then compare those results with those of a sample of 15 spiral galaxies. Their conclusions include the following:

1) Gas-rich lenticular galaxies generally have more rings, both inner and outer, than do spirals. The radii of the outer rings of the lenticulars have values as great as $10R_{25}$ or a bit more.

2) Spiral galaxies do not have large outer rings. Instead, they tend to have Gaussian-shaped HI density profiles that seldom extend beyond $2R_{25}$.

3) The inner rings of both types tend to have the same kinematics as the stellar disk of the host galaxies.

4) In about 1/2 the cases, the outer rings tend to show a distinct disconnect from the host disk/inner ring structures. In those cases, they display quite different kinematics with tilt angles as great as 55˚ relative to the disk.

5) All the outer rings are seen to be rotating and their velocity curves are observed to be flat reminiscent of the star velocity profile in the MW.

6) The total mass of the rings is typically no more than a few percent of the total mass of their host galaxy.

While useful, for our purposes this study does have the limitation that the sample set was chosen to include only gas-rich galaxies so it does not give any indication of what percentage of ETGs contain HI rings. The authors of the next

work, [3], took a different approach. They looked at all ETGs in a volume of space within and surrounding the Virgo cluster with the only criterion being that they had a brightness greater than $M_K = -21.5$. Because their sample set was not restricted to only gas-rich ETGs, their results do indicate what fraction of all ETGs has HI rings. Summarizing their results, we find:

1) The morphology of the gas varies continuously from outside the Virgo cluster across the boundary to inside the cluster; from regular structures to unsettled distributions including tails and systems of clouds.

2) Near the center of the Virgo cluster, the HI detection rate was much lower and the percentage of ETGs with slow rotation rates was much higher.

3) Outside the Virgo group, ~40% of the galaxies host HI structures in some form whereas inside the Virgo group, only ~10% of the galaxies host such structures.

4) The structures within the stellar body of the galaxies (inner rings) had the same kinematics as the body while at least 1/2 of the structures located outside the stellar bodies were found to be kinematically disconnected from the bodies.

5) The outer disks have radii ranging to more than $10R_{25}$.

6) The settled HI systems are observed to be rotating. The periods range from a few hundred Myr for the inner disks to a few Gyr for the outer disks.

7) The mass distribution of HI is much narrower and the peak column densities are much higher for spiral galaxies than they are for lenticular galaxies. ETGs host less HI as a family but there is considerable overlap in the tail of the spiral galaxy distribution.

8) There is no correlation between the masses of the inner and/or outer disks and the stellar mass of the host galaxy.

We note that the results from the two groups are consistent in many respects.

The authors of the next study, [4] examined the effect of the environment on the HI disks of spiral galaxies both nearby and inside the Virgo cluster. They found that the amount of HI in the sampled galaxies decreased steadily from outside to the center of the cluster where the amount was considerably smaller. They also observed many galaxies at intermediate distances from the center with long HI tails pointing away from the center. They suggest that these are HI stripped from the galaxy but we will propose an alternative explanation in what follows.

The previously mentioned sources were primarily concerned with ETGs but we are also interested in the percentage of spiral galaxies that contain measurable amounts of HI. The next work is based on a selection of galaxies taken from the RC3 catalogue, [5]. The catalogue itself reports HI detections for 6090 out of 23022 entries or about 26% with reported HI masses in the range from $2.75\times10^9 M_\odot$ to $20.98\times10^9 M_\odot$. Concerning the remainder, nothing can be said because the catalogue does not differentiate between non-detections and the absence of observations. To remedy this deficiency, the authors of [6] reported on observations of 57 galaxies selected from that catalogue based on their not having reported HI

information. Of this sample, 74% were observed to contain HI with mass totals ranging from $0.04\times10^{9}M_{\odot}$ up to $10.4\times10^{9}M_{\odot}$. If we add the 6090 to 74% of the remainder, we find a value of ~80% for the fraction of spirals that contain measurable amounts of HI.

One thing that the HI systems in all these studies have in common is that there is to some degree, an observed optical counterpart in the outer HI regions, whether in the form of previous or ongoing star formation, the presence of dust, or something else that is a source of optical radiation. What we will review next are very recent results that report the existence of large outer rings (and spheres) that have no optical counterparts, [7] [8] [9]. These structures are at the large end of the size scale of outer rings. A total of 6 such structures have so far been reported; of these, four have an identified host galaxy and the other two do not. Reference [7] reports the discovery of a large "C" shaped HI ring around the galaxy AGC 203001, (A1 for later reference). The long dimension of this structure is ~115 kpc which is about 4 times the radius of the host galaxy. Aside from 5 very small, isolated optical sources, the disk has no optical counterparts.

In references [8] and [9], the authors report the discovery of 5 circular HI regions (ORC's) with no optical counterparts. The authors have established that these sources are both very rare and very large. The most obvious difference relative to the A1 ring is that these all these latter appear as circular structures which, with one exception, have a brighter than expected outer edge indicating that the structures are spherical rather than disk-shaped. This conclusion is supported by the very low probability that a collection of randomly orientated structures with any shape other than spherical would all appear circular. Three of these structures have been associated with *elliptical* host galaxies. ORC1 has a ring size of 510 kpc with a host galaxy size of 39 kpc for a ratio of 13. ORC4 has a ring size of 370 kpc. No size is given for the host galaxy but a comparison of figures 5 and 7 of [8] indicates a size ratio at least as large as that of ORC1. Finally, ORC5 has a ring size of 300 kpc and a host galaxy size of 30 × 18 pc for a ratio ≥ 10. An interesting point is that the morphology of these rings seems to match that of the host galaxy as does that of the A1.

The last ORCs, 2 - 3, are exceptional, first because they are very close together and appear to be related, and second, because, neither separately nor collectively, are they associated with a host galaxy. They are both circular but while ORC 2 has a bright edge suggesting a spherical shape, ORC 3 does not which suggests a disk shape although that is no more than a suggestion. Because of the lack of an associated galaxy, the redshift of these is not known so their size is also unknown.

Finally, we mention the Milky Way. Seen from afar, its HI distribution [10] would appear typical with a total HI mass of $\sim 8\times10^{9}M_{\odot}$. This value falls a little below the midpoint of the range of values reported in RC3. The distribution falls off exponentially with radial distance which is typical of spirals and although gas has been detected out to a distance of $5R_{25}$, that atypically large ex-

tent is probably more a matter of detection sensitivity rather than a reflection of some structural difference between the MW and other spiral galaxies.

To summarize, *outside* galaxy clusters, spirals dominate (they amount to about 77% of all galaxies), and about 80% of the total contain measurable amounts of HI. The radial distributions are generally Gaussian with 2 times the stellar radius being a typical practical cutoff. The ETGs have a much lower percentage of HI content; about 40% verses 80% and instead of a Gaussian distribution of HI, ~47% of the ETGS with HI (~20% of the total) have large outer rings with radii ranging from a few times to as much as 13 times R_{25}. A smaller percentage of ETGs, <10%, have inner rings reminiscent of spiral rings but typically with a much lower total mass. Finally, there are a few cases of HI rings or clouds that do not appear to be associated with host galaxies.

In all these cases, the velocity profiles of the distributions are observed to be flat.

Using the Virgo cluster as our example, inside clusters, ETGs dominate the population and in all cases, the amount of HI associated with all galaxy types is much reduced. From [3], we find the most of the ETGs have no HI and, while spirals do have detectable amounts, the magnitudes are greatly reduced relative to those found outside the cluster, [4].

One striking feature is the universality of it all. The HI structures are far too widespread and have too much in common all across the spectrum of galaxies to be the consequence of random events such as galaxy collisions.

3. Origin of HI Rings

We now come to the new model described in Part 1 which asserts that the result of nucleosynthesis was a gas of protons (and electrons) distributed in space according to a vacuum imprint that defined all structures. Later, at the time of recombination, the protons and electrons combined to form HI. Thus, there is no mystery about the origin of the HI. Aside from small amounts of ^{4}He, there was nothing else. The problem is not accounting for the HI, it is accounting for everything else.

We showed that the critical point in the evolution of cosmic structures was the point at which the influence of the expansion of the universe was counterbalanced by gravitation attraction. At that time, the size of the galaxies reached a maximum and their expansion stopped. We refer to that event as their zero-velocity point (ZVP.) What is interesting from the point of view of outer HI rings is that galaxies reached that point with sizes many times larger than their final size. It follows that they subsequently underwent compaction to reach their present-day size.

The origin of the larger outer rings can now be easily stated. They are outer regions of the original gas cloud that remained in place at the galaxies' maximal size instead of contracting with the inner regions. The range of sizes relative to the present-day sizes of the host galaxies is also easily understood because the

new model predicts a wide range of maximal sizes depending on the size and mass of the galaxy. In Part 1, we gave two examples. The first was the Milky Way (MW) which had a ZVP size equal to 5.2 times its present-day size and the second was a hypothetical dwarf galaxy whose ZVP size was 45.9 times its present-day size.

This disconnection and the fact that ETGs do and LTGs do not exhibit outer rings are clearly critical elements of the whole HI ring problem and it is incumbent on us to show how these could have come about. To study this problem, we consider the equations of motion of a low-density gas cloud undergoing gravitational accelerations only. The required equations are Euler's equation and the equation of continuity. Because the temperature and density were both small at the ZVP when the compaction began, we neglect the pressure gradient term in Euler's equation. We intend only to establish the general character of the initial evolution of the cloud. We assume cylindrical symmetry and consider only radial motion. The proto galaxy was rotating but, because it was the vacuum that was doing the rotating (and carrying the gas along with it), there are no rotation terms in the equations of motion.

After defining dimensionless variables by

$$r = R_0 \bar{r} \tag{3-1a}$$

$$t = t_G \left(1 + \bar{t}\right) \tag{3-1b}$$

$$\rho(r) = \frac{M_G}{R_0^2} \bar{\rho}(\bar{r}) \tag{3-1c}$$

$$v(r) = \sqrt{\frac{GM_G}{R_0}} \bar{v}(\bar{r}), \tag{3-1d}$$

the equations become

$$\frac{\partial \bar{v}}{\partial \bar{t}} + K\left(\bar{v}\frac{\partial \bar{v}}{\partial \bar{r}} - \bar{a}_{disk} - \bar{a}_{Bulge}\right) = 0 \tag{3-2a}$$

$$\frac{\partial \bar{\rho}}{\partial \bar{t}} + K\left(\bar{v}\frac{\partial \bar{\rho}}{\partial r} + \bar{\rho}\frac{\partial \bar{v}}{\partial \bar{r}} + \frac{\bar{\rho}\bar{v}}{\bar{r}}\right) = 0 \tag{3-2b}$$

where K is the dimensionless constant

$$K = \sqrt{\frac{GM_G}{R_0}}\frac{t_G}{R_0}. \tag{3-3}$$

The constant R_0 is the size of the galaxy-to-be at the ZVP, M_G is its mass, and $t_G = 3.2\times10^{16}$ s. The acceleration terms are those of the disk and the bulge respectively. The dimensionless bulge acceleration is just

$$\bar{a}_{Bulge} = -\frac{f_B}{\bar{r}^2} \tag{3-4}$$

where $f_B = M_{Bulge}/M_G$ is the bulge mass fraction. The disk acceleration takes a bit more work. From [11], the potential seen by a test particle in the plane of a thin disk of radius a with a *uniform* surface density of σ is given by

$$V(r,a) = -2G\sigma\left[(a+r)E(k)+(a-r)K(k)\right] \tag{3-5}$$

where $K(k)$ and $E(k)$ are the complete elliptical integrals of the 1st and 2nd kind respectively and

$$k = 2\frac{\sqrt{ar}}{a+r}. \tag{3-6}$$

This potential is defined everywhere in the plane of the galaxy except at the outer boundary, $r = a$.

Since we are interested not in a uniform disc, but one with a varying density, we divide the disk into a series of annuli, each with its own uniform density. The potential due to an annulus of inner radius b is then

$$V(r,a,b) = V(r,a) - V(r,b). \tag{3-7}$$

The acceleration is given by the gradient. Doing the algebra for $V(r,a)$ gives

$$a_a = -\frac{\partial V(r,a)}{\partial r} = \frac{GM_G}{R_0^2}\bar{a}_a \tag{3-8}$$

where the dimensionless acceleration is

$$\begin{aligned}\bar{a}_a = 2\bar{\rho}\Bigg\{E(\bar{k}_a) - K(\bar{k}_a) + \frac{1}{2\bar{r}}\frac{\bar{a}-\bar{r}}{\bar{a}+\bar{r}}\Bigg[(\bar{a}+\bar{r})\left(E(\bar{k}_a) - K(\bar{k}_a)\right) \\ + (\bar{a}-\bar{r})\left(\frac{E(\bar{k}_a)}{1-\bar{k}_a^2} - K(\bar{k}_a)\right)\Bigg]\Bigg\}\end{aligned} \tag{3-9}$$

The acceleration due to an annulus is then the difference

$$\bar{a}_{annulus} = \bar{a}_a - \bar{a}_b. \tag{3-10}$$

The total acceleration of a test particle at position $\bar{r}$ is found by summing over all the annuli. Because the acceleration is singular at the annulus boundaries, we evaluate each annulus at its midpoint.

Except at the ends, the spatial derivatives were approximated by central differences. To account for the fact that the outermost annulus had no material arriving from outside the disk boundary, we needed to adjust the equation for that annulus with the result

$$\frac{\partial\bar{\rho}}{\partial\bar{t}} + K\left(\bar{\rho}\frac{\partial\bar{v}}{\partial\bar{r}}\right) = 0. \tag{3-11}$$

These equations comprise a set of non-linear PDEs. To solve them, we used a predictor-corrector solver known as "Lsoda" which we had on hand from previous work. This solver was developed at the Lawrence Livermore Laboratory several decades ago. It was originally written in Fortran but we ported it to the Microsoft VB.Net platform. This solver automatically switches between Adams-Bashford and Gear Stiff equation methods and automatically adjusts the step size and method order when necessary. Both Fortran and "c" language versions can be found on the internet.

We now have two practical problems to address. Equation (3-2a) is stable but (3-2b) is not. The issue is the term arising from the cylindrical geometry. Separating the last term of (3-2b) we have the truncated equation

$$\frac{\partial \bar{\rho}}{\partial \bar{t}} = \left(K \frac{-\bar{v}}{\bar{r}} \right) \bar{\rho} . \tag{3-12}$$

Because the velocity is always negative, an error of any size in the numerical solution can excite an unphysical exponential increase in the density. To suppress this spurious behavior, we introduced an *ad hoc* damping factor into the equations.

The second problem is that the numerical derivatives of the density tend to be erratic for small $\bar{r}$. In an effort to reduce the impact of this problem, we applied the smoothing procedure described in [12], with a smoothing parameter of $p = 0.3$, to the raw derivatives. Figure 1 shows an example taken at a time of $\bar{t} \approx 1$.

As we often do, we used the MW as our example with a ZVP size multiplier of 5 so $R_0 = 5R_{MW}$ which results in an equation parameter of $K = 0.82$. Because we are beginning the simulation at the ZVP, the initial velocities are zero and we assume an initial constant surface density equal to the disk mass divided by its area.

In Figure 2, we show the results for two values of the bulge mass fraction. We remind the reader that the model is only intended to show the general character of the initial evolution and nothing more.

These results were calculated with both the damping factor and spatial derivative smoothing included. The results are not overly sensitive to the magnitude of the damping as long as it is above a minimum value. The general pattern of the results is similar without the damping but with less stability. The smoothing, on the other hand, had little effect. We ran simulations with and without the

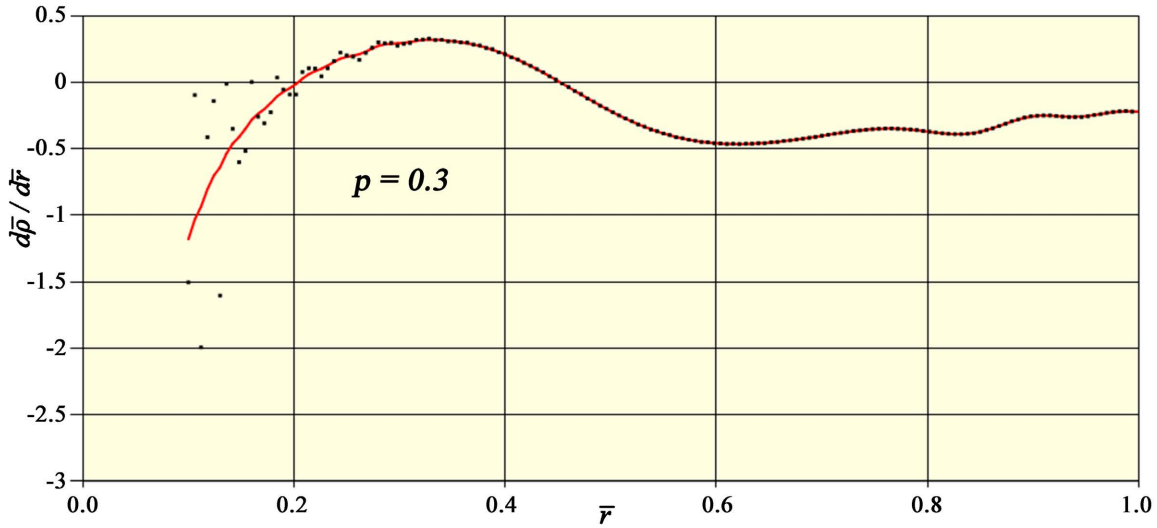

Figure 1. Smoothing of the density spatial derivatives with $p = 0.3$. The black dots are the raw derivatives and the red line is the result of the smoothing.

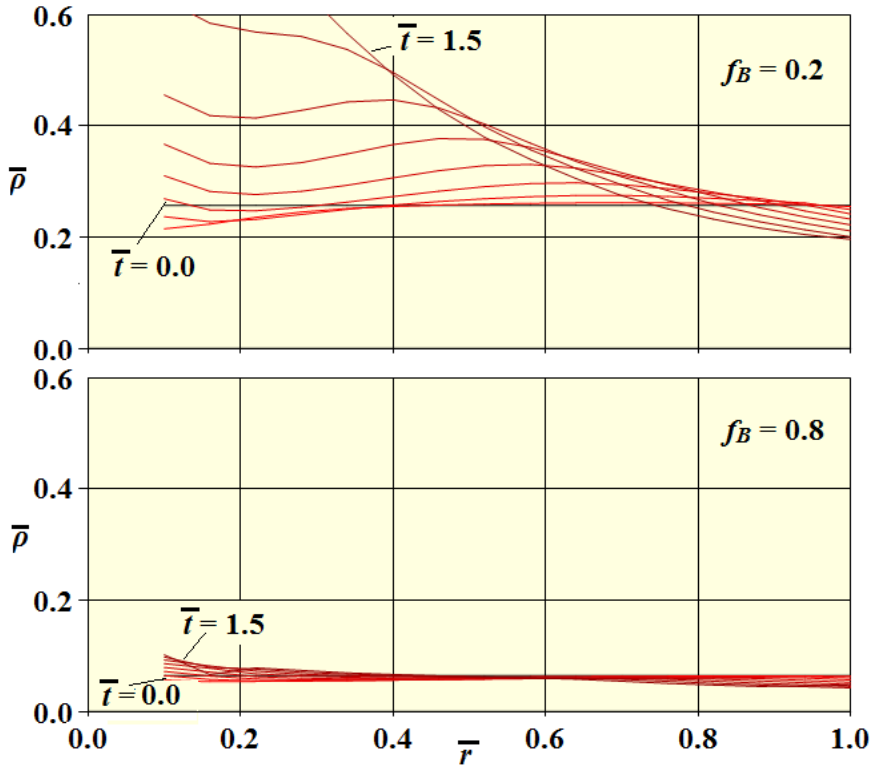

Figure 2. Solution of (3-2) for two values of the bulge mass fraction. Each line represents a different time with the $\bar{t} = 0$ line in black and the later times in red.

smoothing and found essentially no difference in the density distributions despite the scatter shown in Figure 1.

The results for the two cases are dramatically different. With the disk containing most of the mass of the galaxy, we see that, as the evolution proceeds, the outer gas is drawn towards the center with a developing ring structure that also moves toward the center. Recalling that the ZVP size was 5 times the present-day size, we see that by $\bar{t} = 1.5$, the ring structure has already reduced in size to roughly 2.5 times the size of the present-day galaxy. We also see that there is no outer ring.

Turning now to the low-density disk, we find a quite different behavior. In this case, the compacting bulge has much less influence on the disk density so as the bulge shrinks in size, it leaves behind a gas cloud extending out to the original ZVP size or, in other words, an outer ring.

One of the universal of the outer rings is that they are all rotating (see e.g. [1]) and, with one exception, have a flat velocity distribution. (We see from figure 9 of [1] that the HI of the galaxy NGC 3941 had a rapidly rising, linear velocity curve. But this is exactly what one would expect for a system in a rotating vacuum with no residual particle rotation, [13].) We already discussed the flat velocity distribution issue in Part 1 where we showed that both are a consequence of the rotation of the vacuum. We also showed in Part 1 that for the MW, the equivalent particle density of the vacuum energy could be as large as 3.7×10^6

m^{-3} in present-day terms which is close to the mean density of the galaxy. In [13], on the other hand, we showed that, in the case of the present-day MW, a vacuum energy density of about 1% of the galactic matter density is sufficient to balance the inward acceleration due to the galactic matter. Referring back to Figure 2, we see that with the right amount of vacuum energy, the inward flow of the gas in the outer regions would be suppressed and that a disconnection would form at a radial distance of about $\bar{r} = 0.5$. This is somewhat speculative because we don't yet have a complete solution of Einstein's equations including the vacuum energy but for one, the rotation and flat velocity distribution tell us that the vacuum is participating in the dynamics, and second, the necessary magnitude of the density is certainly within the estimated range of possible values. The fact that a balance involving the vacuum energy would be required to form the disconnection could account for the fact that only 47% of ETGs have outer rings. With too little vacuum energy, the bulge will eventually swallow up the entire gas cloud leaving no outer ring behind.

The fact that the kinematics of the outer rings do not necessarily match those of the inner ring and core is understandable. Presumably, as the inner core underwent compaction, some asymmetry in the matter distribution initiated a rotation that was not communicated to the outer ring because of the disconnection.

The general pattern of the results is consistent with observations. LTGs have a high percentage of inner rings and no outer rings. Our model predicts this behavior and the prediction is robust. The calculation for low-mass disk shows first, that the density of outer rings will be low compared to the mass of the host galaxy and second that the probability of forming the disconnection, and hence the outer ring, is less than 100% because a balance between the bulge and the vacuum energy is necessary for it to form.

We can also now understand the gas clouds that are not associated with a host galaxy. These would occur in the rare instances that, first, the vacuum energy density was great enough to prevent any compaction of the gas cloud, and second, that the imprint for the cloud did not contain any star imprints.

For comparison, we consider the solution for a dwarf galaxy. We take as typical values, $M_D = 1.1\times10^{39}$ kg and $R_D = 1.1\times10^{19}$ m. From the galaxy accretion model of Part 1, we find a ZVP size multiplier of 45.9. Putting these together, we obtain an equation constant of $K = 0.77$ which does not differ much from the MW value of $K = 0.82$. That being the case, the calculated dimensionless density curves turn out to be essentially the same. The actual surface densities are given by (3-1c). Putting in numbers, we find that the actual outer ring density for a galaxy with the mass of the MW will be about 5 times greater than that of a typical dwarf galaxy. Also, even though the size multiplier for the dwarf is large, the actual ZVP radii for the dwarf and the MW are must closer, namely 5.05×10^{20} m and 2.47×10^{21} m respectively.

We find that the model can account for the different evolutions of the LTGS

and ETGs and that it is the initial mass distribution rather than the total mass that is the controlling factor.

4. Comparing AGC 203001 with the MW

Aside from their different present-day morphologies, the A1 system mentioned in Section 2 and the MW provide a concrete example that allows us to test the ideas developed in the previous section. Here we show that, because of their similarity in all other respects, it is only their initial distributions of their masses that can explain their different present-day morphologies.

A1 consists of a star-free, "C"-shaped, HI region with a long dimension on the order of 115 kpc that is associated with a SO type galaxy located off-center in the lower arm of the "C". This ring has only a very few isolated optical counterparts which indicate that the original imprint either did not code for stars in the outer regions of the disk or that the imprints dissipated during the expansion phase prior to the ZVP. Both of these galaxies are about 30 kpc in diameter at present and their mass difference is not huge, ($1.5\times10^{10}M_{\odot}$ for A1 and $6.5\times10^{10}M_{\odot}$ for the MW.) They are both disk galaxies but the MW is a barred spiral whereas A1 is lenticular.

The mass of the A1 *ring* is reported to be $\sim 3.4\times10^{9}M_{\odot}$ with the maximum column density measured to be 1.1×10^{24} m^{-2}. The HI content of the MW has a mass of $\sim 8\times10^{9}M_{\odot}$ so again, the difference is not large. Using the accretion model of Part 1, we find ZVP size multipliers of 5.2 for the MW and 3.3 for A1. The difference, in this case, is due entirely to their mass difference since their present-day sizes are the same. Comparing the size of the A1 ring to our estimate of the size of its host galaxy, we find a ratio of about 3.8 which is close to the predicted value of 3.3, a result that supports the validity of our structure evolution model. The authors of [7] do not make any estimate of the thickness of the ring but if we assume a thickness ratio of 1% - 10% which is typical of disk galaxies, we find a proton number density of

$$n_p = 3\times10^{3} - 3\times10^{4}\,\mathrm{m}^{-3}. \tag{4-1}$$

Since the ring has not undergone any compaction, this density is representative of the original density of the proto galaxy.

We now want to compare this with the density of the MW. The volume of the MW is estimated to be about 3.3×10^{61} m^3 and given that its stellar mass is about 1.5×10^{41} kg, we obtain an average particle density of 2.7×10^{6} m^{-3}. For comparison with the A1 ring, however, we really should consider the interstellar medium and that has a present-day value of about

$$n_{ism}(t_0) = 5\times10^{5}\ \mathrm{m}^{-3} \tag{4-2}$$

which is a little less than 20% of the average density. We now use the fact that the MW underwent a compaction of 5.2 to find that its original density would have been on the order of 3.6×10^{3} m^{-3} which is well within the range given in (4-1). It appears then, that both galaxies started with very similar densities of HI

in their outer regions.

Next, we will consider their rotations. The magnitude of the observed velocity of a circular ring tilted relative to the observer by angle, β is given by

$$v = \omega R_r \sin(\beta). \tag{4-3}$$

We now suppose that the observed velocity gradient of the ring given in **Figure 1** of [7] is the consequence of rotation. The radius is about 55 kpc = 1.7×10^{21} m, the velocity magnitude is about 4×10^4 m·s^{-1}, and together, they yield a rotation period of

$$T_r = 7.5 \times 10^9 \sin(\beta) \text{ yr}. \tag{4-4}$$

To get some idea of the tilt angle, we assume that the ring is circular. Comparing the apparent major and minor axes gives us an estimate of $\beta \sim 26^\circ$ which yields a period of

$$T_r \sim 3.4 \times 10^9 \text{ yr} \tag{4-5}$$

which is consistent with the periods of the outer rings of other galaxies reported in the earlier references. The rotating vacuum containing the MW has no angular momentum so its rotation rate would be unaffected by the compaction but the inner portion of the stellar matter does carry angular momentum and so would spin up by a factor of ~5^2 as the galaxy condensed. The present-day rotation period of the MW is about 3×10^8 yr which implies an initial rotation period of ~7.5×10^9 yr. Working in the other direction, starting with (4-5) and using a size ratio of 3.8, we find a present-day rotation period of A1 equal to about 2.4×10^8 yr which is similar to that of the MW.

What we find is that these two systems had similar beginnings. The equation constant for A1 is $K = 0.39$ and while the resulting evolution curves differ in detail from those of the MW, the general character is the same. The conclusion is that the present-day difference in the ring structures of A1 and the MW is a result solely of their initial gas distributions. MW is an example of a high mass disk and A1 is an example of a low mass disk.

5. Presence or Absence of Stars

All the previous arguments involve only average densities so whether some of the matter in each case was in the form of stars is of no consequence as far as the results presented are concerned. The initial distribution of stars was determined by the imprint and if some gas clouds contain few or no stars, that is simply a result of a defining imprint containing no proto star imprints. The fact that the outer disks tend to have low star densities if any at all indicates that the imprints for low-mass disks favored a non-uniform distribution of star templates with stars concentrated towards the center of the resulting proto galaxy.

The reader may have noticed that there is no obvious constraint in the model that would have prevented a widespread distribution of the initial stars throughout the universe. That didn't happen and it is the fractal structure, [13], of the

imprints that is responsible. The fractal structure not only accounts for the filament manifestation of the cosmic web, but it also, through a degree of self-similarity, imposes a hierarchy on cosmic structures. Galaxy clusters formed inside superclusters, galaxies primarily exist inside clusters or groups, and stars are almost exclusively found inside galaxies.

6. Inside Galaxy Clusters

We will now briefly consider the situation within the Virgo cluster. The general picture is that the clusters reached their ZVP at the time, $t = t_G$ consisting of cold neutral hydrogen gas. Soon afterward, galaxies and stars began to form which, in turn, began to release copious amounts of radiation, both inside and outside the cluster, which both ionized and heated the cluster gas. As we saw in Part 1, cluster equilibrium is impossible with radiation so the cluster began to increase in size. The ionization and heating would have applied equally to the galactic HI regions so eventually, there would have been no neutral gas remaining and therefore no distinction between the formerly HI regions and the background. Eventually, as the radiation diminished, the cluster began to contract further heating the gas. The temperature of the now hot gas prevented the gas from recombining with the electrons so the bulk of the gas remained ionized. The same ionization would have occurred everywhere outside the clusters as well as inside but because the outside galaxies were not exposed to the heated cluster gas, the temperature of their gases dropped as the radiation declined which allowed the gas to recombine.

We will now consider the question of the origin of the ETGs that dominate the interior of the Virgo cluster. We showed in Part 1 that the interior ETGs form a distinct population separate from the LTGs. The fact that the stars making up the ETGs were formed before and during the build-up of radiation means that the stars were already formed by the time the gas had reached a high temperature. It follows that ETGs are not LTGs that had stars stripped away because, while the gas might partially scatter a now ionized HI ring, it could not possibly remove stars from a galaxy.

LTGs and a few ETGs inside the cluster are observed to have HI rings but particularly in the case of the LTGs, we showed in Part 1 that these galaxies entered the cluster from outside its boundaries. If the strong radiation was short-lived, then most of these galaxies would have entered the cluster after the burst of radiation diminished. Evidence for this comes from the declining amounts of HI observed in the LTGs as one moves from the outer edge of the cluster to its center, [4].

The authors of [4] also observed large HI tails attached to some LTGs. These are pointing away from the center which is taken as evidence that the galaxies are moving towards the center. The origin of the tails is generally attributed to HI stripping by the cluster gas but we suggest an alternative. The mean free path of the ICM protons is quite large; on the order of the size of a galaxy. In the inte-

rior of a galaxy, the IGM has a higher density so the mean free path will be less but still large. The consequence is that galaxies are porous which makes it unlikely that the ICM could strip sufficient HI to form the tail. What seems more likely is that ICM is cooled sufficiently during its passage through the cold galactic ISM that it combines with the also cooled electrons to form neutral hydrogen. It is cooled ICM that forms the cloud that trails after the galaxy. The time scale for thermalization of the ICM is on the order of 10^8 yr, [14]. In the interior, the density is about 100 times greater than that of the ICM so the time scale will be on the order of 10^6 yr. With a galactic velocity equal to 10^3 km·s^{-1}, the transit time for the ICM would be on the order of $10^{20}\ \mathrm{m}/10^6\ \mathrm{m\cdot s^{-1}} = 3\times10^6$ yr which is about the same so there would be sufficient time for a least a portion of the ICM to undergo recombination. The length of the tails can be estimated in the same manner. With the same velocity, the length will be $l_t = vt_T = 3\times10^{21}$ m which agrees with the observed sizes of the larger tails. Not all galaxies have tails, however, and there could be many reasons for this. First, tails would only be visible for galaxies traveling across the observer's line of sight. Second, tail formation would depend on the passage time of the ICM through the galaxy so galaxies with their disks oriented perpendicular to their direction of travel would be less likely to form tails than would those traveling edge-on to the direction of travel.

We really can't say much more about this evolution without a detailed simulation of the cluster gas beginning at the ZVP and including the radiation. We plan to take up this problem in a future paper.

7. Conclusion

We have shown that the HI rings are the original structures from which the galaxies developed rather than being a consequence of later evolutionary events between established galaxies. We showed that the distinction between the HI rings of LTGs and ETGs is solely a consequence of their original mass distribution and that the disconnection between the inner and outer rings of the ETGs is a result of a balance between the mass of the galaxy disk and the energy density of the vacuum containing the galaxy.

Conflicts of Interest

The author declares no conflicts of interest regarding the publication of this paper.

References

[1] van Driel, W. and van Woerden, H. (1991) Distribution and Motions of Atomic Hydrogen in Lenticular Galaxies XI. A Summary of HI Observations and Evolutionary Scenarios. *Astronomy and Astrophysics*, **243**, 71-92.

[2] Botke, J.C. (2021) A Different Cosmology—Thoughts from Outside the Box. *Journal of High Energy Physics, Gravitation and Cosmology*, **6**, 473-566. https://doi.org/10.4236/jhepgc.2020.63037

[3] Serra, P., *et al.* (2012) The ATLAS Project—XIII. Mass and Morphology of HI in Early-Type Galaxies as a Function of Environment. *Monthly Notices of the Royal Astronomical Society*, **422**, 1835-1862. https://doi.org/10.1111/j.1365-2966.2012.20219.x

[4] Chung, A., van Gorkom, J.H., Kenney, J.D., Growl, H. and Vollmer, B. (2009) VLA Imaging of Virgo Spirals in Atomic Gas (VIVA). I. The Atlas and H I Properties. *The Astronomical Journal*, **138**, 1741-1816. https://doi.org/10.1088/0004-6256/138/6/1741

[5] de Vaucouleurs, G., de Vaucouleurs, A., Corwin, H.G., *et al.* (1991) Third Reference Catalogue of Bright Galaxies. Springer-Verlag, New York. https://doi.org/10.1007/978-1-4757-4363-0

[6] Kamphuis, J.J., Sijbring, D. and van Albada, T.S. (1996) Global HI Profiles of Spiral Galaxies, Astron. *The Astrophysical Journal Supplement Series*, **116**, 15-20.

[7] Bait, O., *et al.* (2020) Discovery of a Large HI Ring around the Quiescent Galaxy AGC 203001. *Monthly Notices of the Royal Astronomical Society*, **492**, 1-7. https://doi.org/10.1093/mnras/stz2972

[8] Norris, R.P., *et al.* (2021) Unexpected Circular Radio Objects at High Galactic Latitude. *Publications of the Astronomical Society of Australia*, **38**, 3. https://doi.org/10.1017/pasa.2020.52

[9] Koribalski, B.S., *et al.* (2021) Discovery of a New Extragalactic Circular Radio Source with ASKAP: ORC J0102-2450. *Monthly Notices of the Royal Astronomical Society*, **505**, L11-L15. https://doi.org/10.1093/mnrasl/slab041

[10] Kalberla, P.M.W. and Kerp, P. (2009) The HI Distribution of the Milky Way. *Annual Review of Astronomy and Astrophysics*, **47**, 27-61. https://doi.org/10.1146/annurev-astro-082708-101823

[11] Lass, H. and Blitzer, L. (1983) The Gravitational Potential Due to Uniform Disks and Rings. *Celestial Mechanics*, **30**, 225-228. https://doi.org/10.1007/BF01232189

[12] Feng, G. (1998) Data Smoothing by Cubic Spline Filter. *IEEE Transitions on Signal Processing*, **46**, 2790-2796. https://doi.org/10.1109/78.720380

[13] Botke, J.C. (2020) A Different Cosmology—Thoughts from Outside the Box. *Journal of High Energy Physics, Gravitation and Cosmology*, **6**, 473-566. https://doi.org/10.4236/jhepgc.2020.63037

[14] Sarazin, C.L. (1988) Mean Free Paths and Equilibration Time Scales. https://ned.ipac.caltech.edu/level5/March02/Sarazin/Sarazin5_4.html